Trend Analysis of Dissipated Electrostatic Discharge Energy in Touchscreen Displays

Zhekun Peng[#1], Shubhankar Marathe[#1], Hossein Rezaei[#1], Giorgi Maghlakelidze[#1], David Pommerenke[#2], Ali Foudazi[#3], Cheung-Wei Lam[#3], Daryl Beetner[#1] and DongHyun Kim[#1],
[1]EMC Laboratory, Missouri University of Science and Technology, Rolla, MO, USA
[2]Graz University of Technology, Graz, Austria
[3]Apple Inc. Cupertino, CA, USA
pengzhe, skmcr4, hrr7d, gmp73, beetner, dkim @mst.edu, david.pommerenke@ieee.org, afoudazi, lam@apple.com,

***Abstract* — Touchscreen displays can be susceptible to spark-less electrostatic discharge events. The energy observed by sensitive touchscreen circuitry can vary significantly with design parameters like the glass thickness, the capacitance between the sensor pad and the ground structure, and the resistance of the traces and sensor terminations connected to the pad. The energy dissipated in resistive structures within the display can lead to damage. Methods are presented to estimate the maximum energy dissipated in the touchscreen circuitry during a spark-less discharge to the display. The trends in the energy with variations in design parameters are analyzed using traditional curve-fitting techniques. The analysis was performed using measured data obtained for 20 touchscreen configurations when the ESD gun was charged to 9 kV and 15 kV. The analysis helps the designer to understand the trends and to predict how future design decisions may impact ESD susceptibility. Results suggest that immunity can be maximized by increasing the glass thickness, reducing the load resistance, and reducing the distance between the sensor pad and the PCB return plane.**

***Keywords* — Electro-static Discharge (ESD), touchscreen, sparkless discharge, energy, measurement-based, trend analysis.**

I. INTRODUCTION

ESD events in touchscreen displays can result in device failures. Typically, IEC 61000-4-2 [1] test is used to evaluate the immunity compliance of the product. Various modeling and measurement methods have been proposed to study the characterization of ESD events [2-6]. The influence caused by different parts of the human body is shown in [2], indicating the effect of the source. A discharge event on the glass may cause current coupling to the touch screen matrix and then to the traces of the IC [3]. From the device perspective, the capacitance between a mobile device and a metallic coupling plane strongly affects the discharge current [4]. The charge, the discharge position, the cleanliness of the screen and the discharge polarity show a strong influence on the discharge to display screens, as well [5]. Most of these parameters, however, only indirectly impact the ESD event. For an in-depth analysis of an ESD event, energy, fields, voltage peak, current peak and the rise time of the ESD pulse should be analyzed. The total dissipated ESD energy is particularly important in some products [7]. In the study presented here, methods are developed to predict the energy delivered to the load resistor of a touchscreen sensor during a spark-less discharge to the display. The highest priority was placed on predicting the energy since it is expected that a high energy discharge is likely to damage the device.

A model for spark-less discharge to displays has been proposed in [8]. This model takes into account the display glass, the PCB design, and the load. The ESD energy dissipated on the display screen is highly dependent on the design configuration. The number of prototype iterations required to predict maximum ESD induced energy should be minimized with minimum cost and time. Therefore, prediction of the maximum dissipated ESD energy through modeling is a critical design requirement. In this paper, a method to characterize and predict the maximum dissipated ESD energy within a specified range of design parameters is proposed.

II. DISCHARGE CHARACTERIZATION METHODOLOGY

A. Design of the Device Under Test (DUT)

A real display contains the glass, the inside PCB and the load. The PCB designed to mimic a touchscreen display sensor was created with a 6x6 matrix of metal patches placed under the display glass as shown in Fig. 1. Each patch is connected to a load resistor (330 Ω~ 56 kΩ) and to an oscilloscope to allow the current to each load to be measured. This resistance is equivalent to the load seen in a touchscreen display sensor circuit. As shown in the Fig. 1, Patch 04, Patch 10 and Patch 16 are in the same column. The patches are tightly pressed against a glass interface using a vacuum, as shown in Fig. 2. The ESD gun is set in air-discharge mode and placed to directly hit the glass above Patch 16 (the center patch). The ESD event occurs on the glass surface. A portion of the discharge current (the portion of interest) goes through a path between the glass surface and the patch, through a via under the patch, and through a resistor on the back of the PCB. A coaxial cable is attached to connect the PCB to an oscilloscope and measure the ESD induced voltage. The voltage can be converted to current by dividing the scope channel input impedance and energy can be calculated based on the current waveform. The other patches are terminated with 50 Ω resistors after the load resistor, the same as the input impedance of the oscilloscope.

Three design parameters are considered during testing. Fig. 3 provides a cross-sectional illustration of the ESD current path during discharge and each of the following parameters:

1. **C_{sp}** - capacitance from the "conductive" layer of ionized air on the glass surface, created by the corona discharge, to the sensor patch on the PCB. The value of this capacitance is determined by the thickness of the glass and its dielectric properties. Three different thicknesses are used: 0.6 mm,

0.9 mm and 1.6 mm. The capacitance values of C_{sp} are 650 fF, 430 fF and 125 fF, respectively.

2. **C_{pg}** - capacitance from the patch to the return plane (ground) of the test PCB. This capacitance is defined by the four-layer PCB manufacturing process. To achieve a low capacitance from the patches to the ground, the ground fill in Layer 2 and Layer 3 is completely removed. Both layers are still kept for thickness requirement. In addition, the ground fill in Layer 4 is partially removed to tune the value of C_{pg}. Values of 485 fF, 2900 fF, 15900 fF and 29900 fF have been investigated.
3. **R_{total}** - total resistance of the sensor trace and termination, here the oscilloscope's input resistance (50 Ω) plus the added resistor ($R_{total} = R_{MELF} + R_{OSC}$). The values of R_{total} investigated in this work are: 380 Ω, 4.75 kΩ, 10 kΩ, 15 kΩ and 56 kΩ.

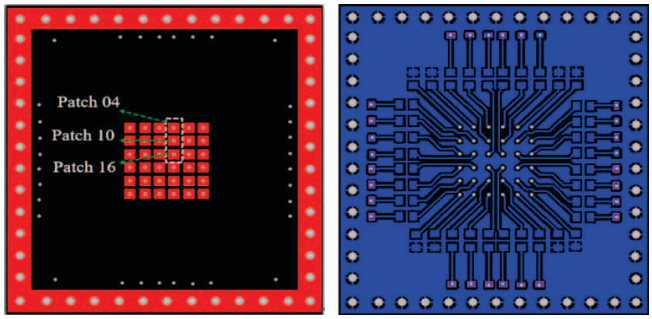

Fig. 1. PCB design of DUT: left - top view, right - bottom view. The glass is pressed against the top layer. On the bottom, the resistors are soldered to traces connected to a coaxial cable on the oscilloscope.

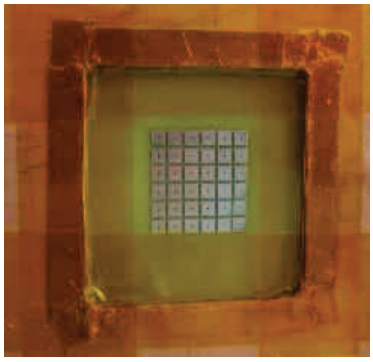

Fig. 2. Photo of glass pressed against the patches. The ESD gun in air discharge mode hits the surface of the glass. The current induced in each patch flows through a resistor on the other side of the PCB.

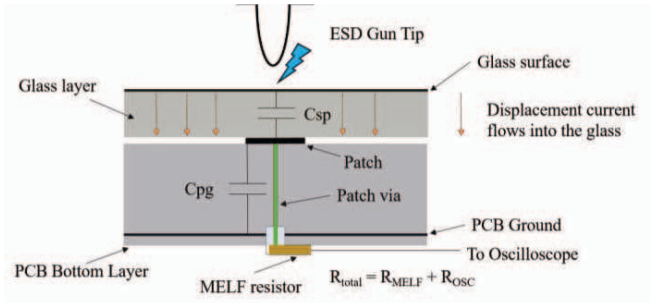

Fig. 3. Schematic illustration of a cross-section of the test PCB. As the ESD gun approaches the glass, a corona is initiated between the ESD gun tip and the glass surface. The surface is charged and a current is induced through C_{sp}. The capacitor C_{pg} will then be charged and the energy will finally be dissipated in the load resistance, R_{total}.

B. Measurement Setup and Automation Algorithm

Fig. 4 describes the test system. The measurement control algorithm is illustrated in Fig. 5. Two motors controlled the movement of the ESD gun. A vacuum pump was used to avoid a gap between the glass and the PCB. An air conditioner and a humidifier were used to control the temperature and humidity of the test environment. An ionizer was used to equalize charges after a discharge to the glass. The PC controlled the scope and the ESD gun movement via an Arduino MCU. The approach speed of ESD gun was fixed at 0.3 m/s.

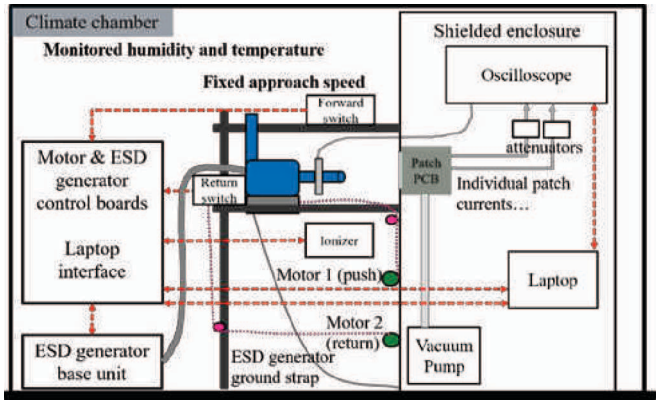

Fig. 4. Schematic diagram of the automated measurement setup. Two motors control the movement of the ESD gun. A vacuum pump, an air conditioner and a humidifier are used to stabilize the test environment.

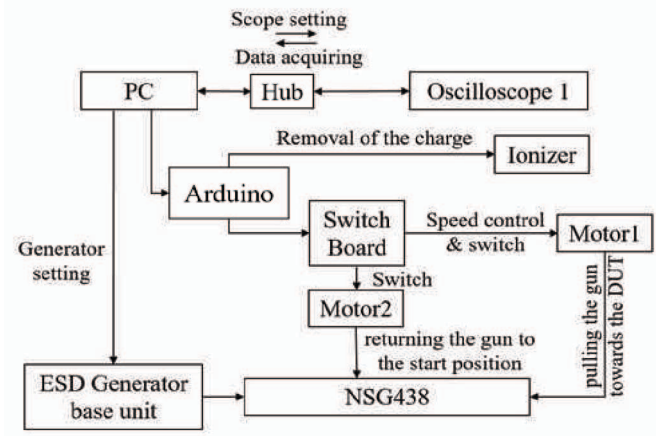

Fig. 5. Flow chart of the measurement control algorithm. The PC controls the ESD generator, the measurement equipment and the Arduino MCU. The MCU is used to control the push/pull motors and the ionizer.

The oscilloscope and other measurement equipment were placed in a shielded cabinet to prevent direct coupling from the ESD gun to the measurement system. The temperature was limited to be within 23.9 °C ~ 26.7 °C, and the relative humidity was limited to be within 30% ~ 35%. This reduced the variability of the ESD discharges.

A current clamp, having 1 Ω transfer impedance, captures the ESD gun discharge current. To capture data the gun is energized and moved towards the glass above the center patch of the DUT. When the gun tip is close enough to the glass, but prior to touching it, a discharge from the gun tip to the glass surface will initiate the surface corona on the glass surface.

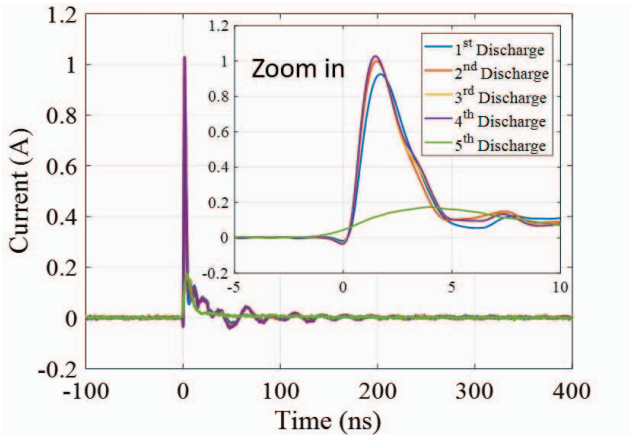

Fig. 6. Worst case current waveforms through the center patch for the following configuration: ESD gun voltage = 9 kV, C_{sp} = 430 fF, C_{pg} = 2900 fF, R_{total} = 380 Ω. Apart from the fifth discharge, the other curves show reasonable repeatability with less than a 20% deviation in peak, rise time and energy.

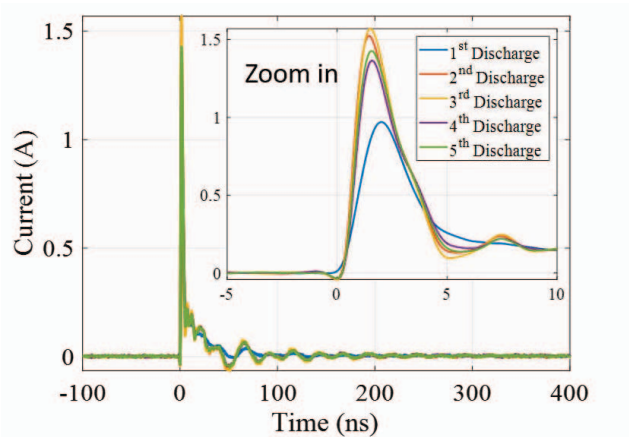

Fig. 7. Worst case current waveforms through the center patch for the following configuration: ESD gun voltage = 15 kV, C_{sp} = 430 fF, C_{pg} = 2900 fF, R_{total} = 380 Ω. Apart from the first discharge, the other curves show reasonable repeatability with less than a 20% deviation in peak, rise time and energy.

The oscilloscope was used to measure the voltage waveform. One or two 20 dB attenuators protect the oscilloscope against the current from the ESD gun. The ESD gun is set to air discharge mode at 9 kV or 15 kV.

C. Calculation of the Maximum Dissipated Energy

Each time the gun approaches the glass, multiple current pulses are detected. This indicates that the surface corona process will not reach an equilibrium after the first discharge [9-10]. As energy is selected as a merit for damage to the display, the discharge having the largest energy is selected.

The energy of each event is calculated as:

$$Energy = R_{total} * \int_{t_{start}}^{t_{stop}} I^2 dt \qquad (1)$$

where t_{start} and t_{stop} are the start and stop time of the event.

To take into account variations that may be caused by the environment, by spark development, by corona development or by mechanical issues, each configuration (defined by a certain combination of C_{sp}, C_{pg} and R_{total}, and discharge voltage) was measured five times. The largest current waveform among the five discharges for each configuration was selected to obtain the maximum energy dissipated in R_{total} for the selected configuration.

III. Measurement Results

A. Air Discharge Repeatability

Fig. 6 and 7 show the waveforms for the worst events for C_{sp} = 430 fF, C_{pg} = 2900 fF and R_{total} = 380 Ω as an example to illustrate the repeatability.

In Fig. 6, except for the fifth discharge, the current peaks are in the range of 0.93 A ~ 1.03 A, the rise time is in the range of 0.75 ns ~ 0.89 ns, and the energy is in the range of 0.65 μJ ~ 0.74 μJ. In Fig. 7, except for the first discharge, the peaks of the rest tests are in the range of 1.36 A ~ 1.57 A, the rise time is in the range of 0.72 ns ~ 0.75 ns, and the energy is in the range of 1.44 μJ ~ 1.73 μJ.

B. Histogram of maximum dissipated energy

The load current was measured during a spark-less discharge to a total of 20 configurations when the ESD gun voltage was 9 kV and 15 kV. Histograms of the peak energy found for each of these configurations are shown in Figs. 8 and 9. The order of the cases is set according to the maximum dissipated energy at 15 kV. The overall trends shown in Fig. 8 and Fig. 9 are comparable. The noticeable difference between the two figures is the range of dissipated energy. At 9 kV, the range of the energy is 0.04 μJ ~ 29.2 μJ. At 15 kV, however, the energy varies from 0.2 μJ to 14662.6 μJ.

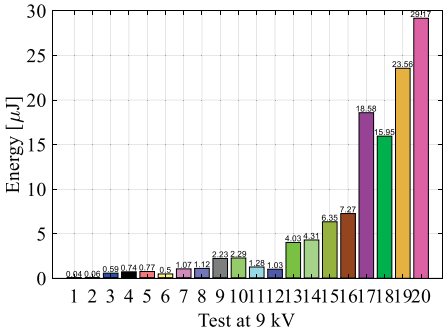

Fig. 8. Histogram for maximum dissipated energy when the ESD gun was set to 9 kV (linear scale).

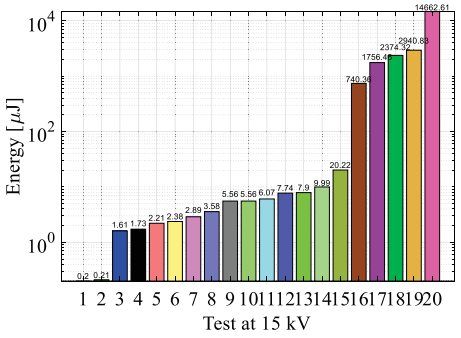

Fig. 9. Histogram for maximum dissipated energy when the ESD gun was set to 15 kV (log scale).

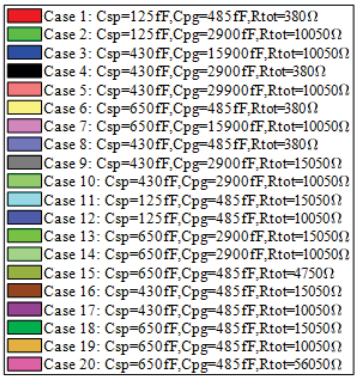

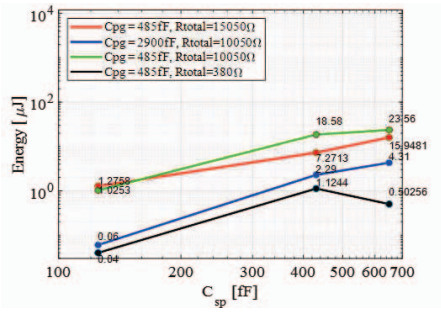

Fig. 10. Trends for maximum Energy vs. C_{sp} when the ESD gun was charged to 9 kV. Design parameters C_{pg} and R_{total} are varied. Overall, the energy increases with C_{sp}.

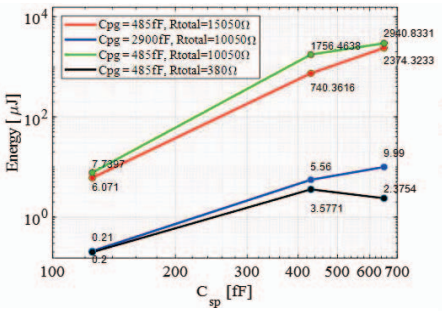

Fig. 11. Trends for maximum Energy vs. C_{sp} when the ESD gun was charged to 15 kV. Design parameters C_{pg} and R_{total} are varied. Overall, the energy increases with C_{sp}.

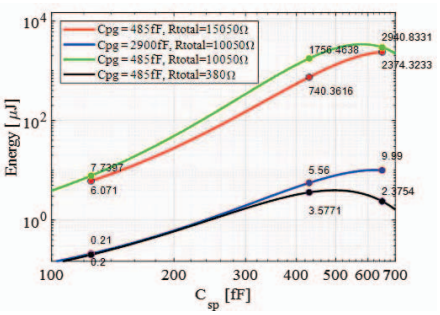

Fig. 12. Gaussian Fit of trends when the ESD gun was charged to 15 kV. The fit is reasonable within the test case range.

From the histograms, one can find the maximum dissipated energy for the measured configurations and determine if the display circuit can withstand the energy. No single parameter dominates the behavior. To determine the energy dissipated in a case not studied here requires additional information. Trend analysis and prediction are investigated in the next section for this purpose.

IV. Methodology of Trend Analysis For The Design Parameters

Results from the tested cases can be divided into several sub-data sets to study the effect of each design parameter. For example, for the analysis of the effect of C_{sp} on the maximum ESD induced energy, a sub-data set with different combinations of fixed C_{pg} and R_{total}, can be plotted with respect to varying values of C_{sp} to visualize the effect of C_{sp}. The measurement points can be interpolated to roughly predict the maximum energy induced at intermediate points. As linear interpolation was often insufficient, a curve fitting method was also used to generate a function that can approximately predict the maximum ESD energy from the limited set of data points.

A. Trend analysis on the effect of the capacitance from the surface to patch (C_{sp})

The approaching ESD gun charges the surfaces of the glass. The value of C_{sp} is dependent on the thickness of the glass. Larger glass capacitance leads to higher ESD currents from the source, and the wider spreading of the corona on the glass. Compared with the energy histogram, it can be concluded that thinner glass thickness typically leads to more energy dissipated in the resistor.

The trend in maximum dissipated energy generated by four combinations of C_{pg} and R_{total} are shown in Figs. 10 and 11. All four curves show an ascending trend; however, the gradient sometimes decreases as C_{sp} increases. In general, if C_{pg} is relatively small and C_{sp} is relatively large, the energy is higher. This combination should generally be avoided.

An attempt to fit these trends was made using an Exponential, Power, Polynomial, Gaussian, Rational, Fourier and Log Function. Among them, the Gaussian function fit the trends best. The Gaussian approximation of the trends are shown in Fig. 12.

B. Trend analysis on the effect of the capacitance from the patch to ground (Cpg)

The capacitor from the patch to ground (C_{pg}) works as a charge storage. It is parallel to R_{total}. Regardless of the increase in the capacitance, all the charge stored in C_{pg} will be dissipated at R_{total}. The amount of energy dissipated, however, may depend on other circuit parameters and on the event itself. Making several measurements to get the maximum dissipated energy from the worst event is still needed.

Figs. 13 and 14 show the trend in the maximum energy with C_{pg} for two combinations of C_{sp} and R_{total} and for ESD charge voltages of 9 kV and 15 kV. Overall, the plots show a descending trend in the dissipated energy with increasing values of C_{pg} in the range of 485 fF $\leq C_{pg} \leq$ 29.9 pF. There is a slight increase in energy for high values of C_{pg}. If C_{pg} is fixed, a larger C_{sp} leads to more dissipated energy, which is the same

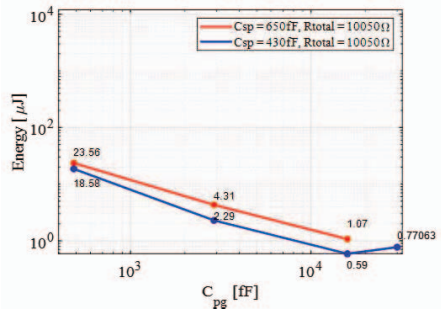

Fig. 13. Trends for maximum Energy vs. Cpg when the ESD gun was charged to 9 kV. Design parameters C_{sp} and R_{total} are varied. Overall, the trend shows energy decreases as Cpg increases.

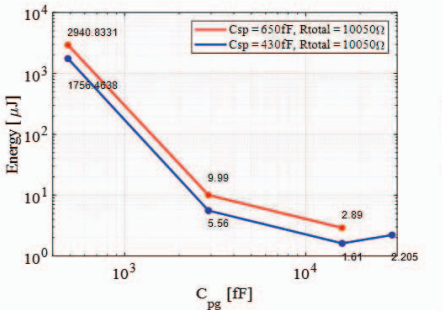

Fig. 14. Trends for maximum Energy vs. Cpg when the ESD gun was charged to 15 kV. Design parameters C_{sp} and R_{total} are varied. Overall, the trend shows energy decreases as Cpg increases.

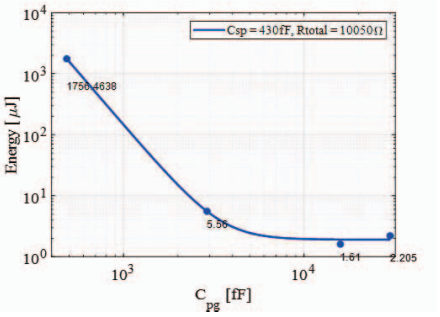

Fig. 15. Power Function Fit of the maximum Energy vs. Cpg when the ESD gun was charged to 15 kV. The model works well within the test case range.

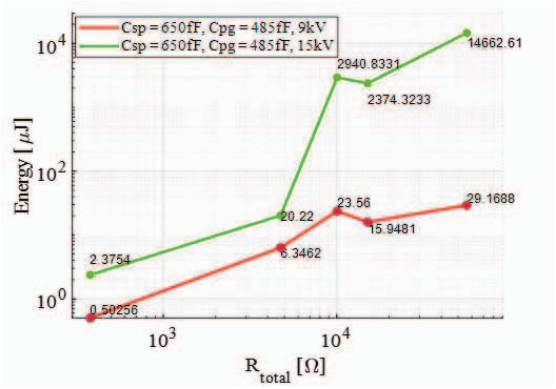

Fig. 16. Trends for maximum Energy vs. R_{total} when the ESD gun was charged to 9 kV and 15 kV. The curve shown has the most data points among all the curves. Overall, it shows an ascending trend as R_{total} increases.

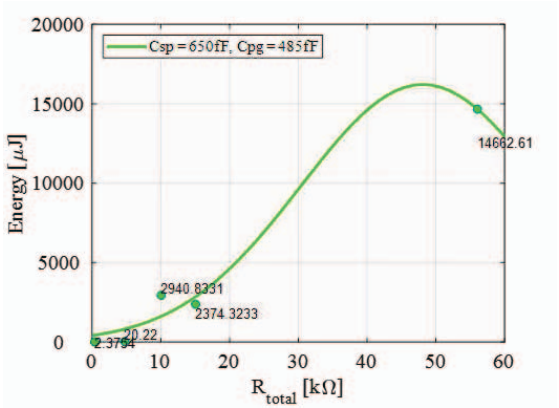

Fig. 17. Gaussian Fit for results when the ESD gun was charged to 15 kV. The model works within the test case range.

result observed in the previous discussion. These figures show that a smaller C_{pg} results in larger dissipated energy, but including configurations 1, 6, 8, 11, 12, and 15 shows that C_{sp} and R_{total} also influence results. The trends in Figs. 13 and 14 also suggest that a parasitic capacitance associated with the load resistance, R_{total}, might effectively increase the value of C_{pg} and cause an unexpected decrease in the dissipated energy.

These trends were fit with an Exponential, Power, Polynomial, Gaussian, Rational, Fourier and Log Function. The Power function fit the measured points best to show a rough trend of C_{pg}. The fitted plot is shown in Fig. 15.

C. *Trend analysis on the effect of the load resistance (R_{total})*

As shown in Fig. 16, the dissipated energy is roughly linear with the size of the load resistance, R_{total}, over the measured range. The slope is different for the 9 kV tests compared to the 15 kV tests. The change in slope may be related to the change in circuit parameters associated with the spark-less discharge, like the conductivity of the ionized layer on the surface of the glass or of the charge transport mechanism between the glass and the gun. The physical effect, such as corona on the PCB surface, or breakdown in the resistors may also explain the result. Different behavior would be expected for larger values of R_{total}, as the dissipated energy is not expected to increase ad infinitum. The fitting curve, therefore, should be increasing at the beginning, until a certain point stops increasing. More points should be measured to more accurately predict behavior outside of the given range.

For the points shown in Fig. 16, the Gaussian function fit the curve best. The fitted curve is shown in Fig. 17.

V. Discussion

The proposed method to characterize the energy delivered by a spark-less discharge to a touchscreen display has the potential to help designers evaluate ESD robustness in cases when the discharge source model is partially unknown and a full-wave or an equivalent circuit model is not available. The trend analysis uses a limited number of measured data points and provides a mathematics-based prediction for intermediate points not contained in the measurement set. This analysis, however, has several limitations as discussed below:

1. **The complexity of the measurement setup.** Each test configuration requires two or three days to measure and analyze, which in practice limits the number of obtainable data points. This directly impacts prediction quality, as the method fits curves to empirical data. The scarcity of data points leads to a loss of accuracy.
2. **The prediction assumes a stable environment.** Even though the humidity, the temperature, and the approach speed are stabilized, measurement repeatability is less than 20%. The limited repeatability is due in part to the expected statistical variations in the spark-less discharge event. Nevertheless, the predictions follow a trend and can be used to estimate the maximum dissipated energy.
3. **The model is empirical.** That is, the models are not physics-based, but rather rely heavily on curve fitting and measured data. On the other hand, this property can be considered an advantage, since no rigorous physical model is required. Creating a detailed model is possible and depends on two parts: a) an equivalent circuit of the structure of the screen and the PCB, and b) a source model for the ESD generator as it discharges to the surface of the glass.
4. **The model accuracy is limited by the range of the tested design parameters.** Outside the dataset used for trend analysis, the model loses accuracy and cannot be used for outcome prediction.
5. **The model is data-sensitive.** It has been observed that high energy levels starting from Configuration 16 at 15kV may result from the measurement setup, or an additional discharge event, such as corona on the PCB surface, or sparking along the resistors. Physical analysis is needed to determine the overall trend.

VI. Conclusion

A novel method for characterizing spark-less discharge to touchscreen displays has been developed. Unlike the resource-heavy and rigorous physics-based models, it requires no detailed analysis of the structure. The approach consists of performing a trend analysis on measured dataset for pre-determined values of design parameters. A total of 20 design configurations were measured and analyzed for two different

ESD gun voltages. The method predicts trends in the maximum energy dissipated in the touchscreen circuits during an ESD event and helps to understand the impact of design variations.

The trends show that in order to minimize the maximum dissipated energy, one must minimize R_{total} and C_{sp} and maximize C_{pg}. In order to reduce C_{sp}, the glass should be made thicker. Increasing C_{pg} requires a shorter distance between the patches and PCB ground (i.e. a thinner inner dielectric layer).

This method can be used in conjunction with a physics-based full-wave model. Such a model can be used to calculate a handful of data points, and combined with the measurement dataset in order to increase the prediction accuracy. Once a sufficiently large dataset is obtained, there is no longer a need to run an extensive full-wave calculation, as the proposed model can be used to predict the maximum dissipated ESD energy. This application is a subject for the future research.

VII. Acknowledgment

This paper is based upon work supported partially by the National Science Foundation under Grant No. IIP-1916535.

VIII. References

[1] Electromagnetic Compatibility (EMC)—Part 4-2: Testing and Measurement Techniques—Electrostatic Discharge Immunity Test, IEC International Standard 61000-4-2, 2007.

[2] T. Ishida, S. Nitta, F. Xiao, Y. Kami and O. Fujiwara, "An experimental study of electrostatic discharge immunity testing for wearable devices," *2015 IEEE International Symposium on Electromagnetic Compatibility (EMC)*, Dresden, 2015, pp. 839-842.

[3] S. Shinde et al., "ESD to the display inducing currents measured using a substitution PC board," *2016 IEEE International Symposium on Electromagnetic Compatibility (EMC)*, Ottawa, ON, 2016, pp. 707-712.

[4] J. Zhou *et al*., "IEC 61000-4-2 ESD test in display down configuration for cell phones," *2016 IEEE International Symposium on Electromagnetic Compatibility (EMC)*, Ottawa, ON, 2016, pp. 713-718.

[5] A. Talebzadeh, Y. Gan, K. Kim, Y. Zhang and D. Pommerenke, "Spark-less electrostatic discharge (ESD) on display screens," *2015 IEEE International Symposium on Electromagnetic Compatibility (EMC)*, Dresden, 2015, pp. 1284-1289.

[6] Z. Zhang, L. Zhang, Z. Sun, N. Erickson, R. From and J. Fan, "Solving Poisson's Equation using Deep Learning in Particle Simulation of PN Junction," *2019 Joint International Symposium on Electromagnetic Compatibility, Sapporo and Asia-Pacific International Symposium on Electromagnetic Compatibility (EMC Sapporo/APEMC)*, Sapporo, Japan, 2019, pp. 305-308.

[7] H. S. Silva, D. F. L. Pereira, E. V. Falcão, H. E. Querino de Carvalho and V. V. Freire, "Electrostatic energy: A possible source of interference," *2015 IEEE International Conference on Microwaves, Communications, Antennas and Electronic Systems (COMCAS)*, Tel Aviv, 2015, pp. 1-4.

[8] Y. Gan *et al*., "Experimental Characterization and Modeling of Surface Discharging for an Electrostatic Discharge (ESD) to an LCD Display," in *IEEE Transactions on Electromagnetic Compatibility*, vol. 60, no. 1, pp. 96-106, Feb. 2018.

[9] S. Marathe, H. Rezaei, D. Pommerenke and M. Hertz, "Detection methods for secondary ESD discharge during IEC 61000-4-2 testing," *2017 IEEE International Symposium on Electromagnetic Compatibility & Signal/Power Integrity (EMCSI)*, Washington, DC, 2017, pp. 152-157.

[10] S. Marathe, G. Maghlakelidze, H. Rezaei, D. Pommerenke and M. Hertz, "Software-Assisted Detection Methods for Secondary ESD Discharge During IEC 61000-4-2 Testing," in *IEEE Transactions on Electromagnetic Compatibility*, vol. 60, no. 4, pp. 1129-1136, Aug. 2018.